

Size effects in the giant magnetoresistance of segmented nanowires

M. Ye. Zhuravlev,^{1,*} H. O. Lutz,¹ and A. V. Vedyayev^{2,†}

¹Fakultät für Physik, Universität Bielefeld, 33501 Bielefeld 1, Germany

²CEA/Département de Recherche Fondamentale sur la Matière Condensée, SP2M/NM, 38054 Grenoble, France

(Received 18 December 2000; revised manuscript received 25 January 2001; published 3 April 2001)

We calculate the resistivity and giant magnetoresistance (GMR) of a segmented nanowire consisting of two ferromagnetic segments separated by a thin paramagnetic spacer. Spin-dependent surface electron scattering is taken into account. The quantization of the electron motion due to the small nanowire cross section leads to oscillations of the resistivity and the GMR. The interplay between spin-dependent electron scattering in the bulk and the surface results in a complex behavior of the GMR as a function of nanowire radius and surface-potential strength. Both increase and decrease of the GMR can be obtained as the spin-dependent surface scattering grows.

DOI: 10.1103/PhysRevB.63.174409

PACS number(s): 73.40.-c, 75.70.Pa

I. INTRODUCTION

The giant magnetoresistance (GMR) has attracted considerable attention since its discovery¹ (various aspects of the subject are, e.g., presented in Ref. 2). The most extensively studied objects of this type are multilayers (see Refs. 3–7 for a theoretical analysis of the GMR). Meanwhile, the successive miniaturization of technical elements require the study of systems whose lateral extension is limited, too. It is therefore natural to consider segmented nanowires consisting of two ferromagnetic parts separated by a thin paramagnetic spacer. The recent development in the research of magnetic nanowires has been reviewed in Ref. 8. In particular, experimental data concerning the GMR in multilayered (segmented) nanowires of about 400-Å radius were discussed in the framework of the quasiclassical Valet-Fert model.³ In a realistic treatment of the transport properties of nanowires the influence of the surface roughness on the electron transport must be taken into account. While this effect has been included in quasiclassical theories,⁹ it has not yet been investigated in detail in quantum-statistical calculations (cf., e.g., Ref. 10).

In this paper we develop a quantum-statistical theory of the GMR in segmented cylindrical nanowires with spin-dependent electron scattering at the lateral interfaces. Specifically we investigate the electron transport along the nanowire axis, in analogy to the current perpendicular to planes geometry in laterally infinite multilayers.

In the current literature on the theory of spin-dependent transport in spin valve structures two approaches are widely presented. One of them uses the simple free-electron model and is able to give a transparent description of the physical phenomena; the other one relies on an *ab initio* calculation of the realistic band structure and gives the result in terms of numerical simulations. Both approaches are complementary to each other. In the work presented in this paper, we follow Refs. 6 and 7 and use the free-electron model, taking into account the exchange splitting of the *d* band. The *s-d* scattering leads to different values for the elastic mean free path of “up-” and “down-” spin *s* electrons. Recent calculations^{11–15} employing realistic band structure have shown that a correct description of GMR can be achieved if

sp-d scattering is allowed for. As in earlier work⁷ we assume that *s* electrons give the main contribution to the current due to their low effective mass if compared to the effective mass of the almost localized *d* states.¹⁶ The mean free path of the conduction *s* electrons depends on the spin due to *s-d* scattering and the different density of states (DOS) of the *d* electrons at the Fermi level. We calculate the mean free paths in the framework of the coherent potential approximation, using the main conclusion of Ref. 17 that the effective mean free paths $l^{\uparrow,\downarrow}$ of the *s* electrons are proportional to the DOS $\rho_{d\uparrow,\downarrow}$ of the *d* electrons (the arrows indicate the spin direction).

As conventionally done in the calculation of bulk scattering, we describe the surface spin-dependent electron scattering by a complex effective surface potential in full analogy with interface scattering in multilayers.¹⁸ The imaginary part of the spin-dependent surface coherent potential V^σ may be defined as

$$\frac{2M \operatorname{Im} V^\sigma}{\hbar^2} = k_F a_0 / \lambda^\sigma,$$

where a_0 is the lattice constant, k_F is the Fermi momentum for electrons with spin projection σ , and λ^σ has the dimensions of a length. Therefore in these units the strength of the diffusive surface scattering can be as large as k_F . It was shown (though for a metal-metal interface)¹⁹ that under certain conditions the ratio $(\lambda^\uparrow/\lambda^\downarrow)$ of surface spin-dependent scattering may far exceed the one for bulk scattering.

In Sec. II we describe briefly the construction of the Green function for a segmented nanowire with spin-dependent diffusive surface scattering of electrons. In Sec. III we calculate the conductivity and the GMR on the basis of the Kubo formalism, and in Sec. IV the transport properties of the segmented nanowire with special attention to the interplay between bulk and surface electron scattering is discussed.

II. GREEN FUNCTION

The Kubo formalism will be used to calculate the conductivity of the segmented nanowire. Following the general

scheme developed in Ref. 6 we start our consideration with the calculation of the one-electron Green function $G^\sigma(\vec{r}, \vec{r}')$ for a segmented cylindrical nanowire of radius R_0 and segment length c_j ($j=1,3$ for the ferromagnetic segments and $j=2$ for the paramagnetic spacer). The Green function obeys the following equation in the j th segment:

$$\left(\frac{\partial^2}{\partial r^2} + \frac{1}{r} \frac{\partial}{\partial r} + \frac{1}{r^2} \frac{\partial^2}{\partial \theta^2} + \frac{\partial^2}{\partial z^2} + E^{j\sigma} - \frac{2M}{\hbar^2} V^{j\sigma} \delta(r-r_0) \right) \times G^\sigma(\vec{r}, \vec{r}') = \frac{2Ma_0}{\hbar^2} \frac{\delta(r-r')}{r} \delta(\theta-\theta') \delta(z-z') \quad (1)$$

and must fulfill the boundary condition

$$G^\sigma(r=R_0, r', z, z', \theta, \theta') = G^\sigma(r, r'=R_0, z, z', \theta, \theta') = 0.$$

We use cylindrical coordinates, with z pointing along the nanowire axis. M is the mass of an electron, a_0 is the lattice constant, and $r_0=R_0-a_0$. The complex parameter $E^{j\sigma}$ depends on the segment j ; it is given by

$$E^{j\sigma} = \frac{2ME}{\hbar^2} + (k_F^{j\sigma})^2 + i \frac{2k_F^{j\sigma}}{l^{j\sigma}}, \quad (2)$$

where E is the energy relative to the Fermi energy, $l^{j\sigma}$ is the mean free path, and $k_F^{j\sigma}$ the Fermi momentum of electrons with spin projection σ in the j layer. The real part of the bulk coherent potential is included in the Fermi energy. Both the d - and the s -electron Green functions obey Eq. (1). We suppose that the spin splitting of the s band is negligibly small. The effective surface potential $V^{j\sigma}$ can be calculated in the coherent-potential approximation similarly to the bulk coherent potential;⁶ thus it has a nonzero imaginary part that defines the diffusive scattering of the electrons. It depends on the segment and the electron-spin direction, but it is constant within a given segment and for a given electron-spin projection. The surface potential is positioned inside the wire at a distance of one lattice parameter from the nanowire surface. An eigenfunction expansion is used to construct the Green function. Starting with the expansion in θ variables,

$$G^\sigma(\vec{r}, \vec{r}') = \sum_n G_n^\sigma(r, r', z, z') e^{in(\theta-\theta')}, \quad (3)$$

$G_n^\sigma(r, r', z, z')$ obeys the equation

$$\left(\frac{\partial^2}{\partial r^2} + \frac{1}{r} \frac{\partial}{\partial r} - \frac{n^2}{r^2} + \frac{\partial^2}{\partial z^2} + \frac{2M}{\hbar^2} E - \frac{2M}{\hbar^2} V^{j\sigma} \delta(r-r_0) \right) \times G_n^\sigma(r, r', z, z') = \frac{2Ma_0}{\hbar^2} \frac{\delta(r-r')}{r} \delta(z-z'). \quad (4)$$

Since the imaginary part of the surface potential $V^{j\sigma}$ shall be nonzero, we deal with a non-self-adjoint boundary problem. In that case one can use a biorthogonal expansion to construct the solution of the corresponding problem.²⁰ The

eigenfunctions $\phi_{nm}^{j\sigma}(r)$ of the problem (4) are expressed through the Bessel function of the first and the second kind. These eigenfunctions are different in the different segments. The Green function then takes the form

$$G^\sigma(\vec{r}, \vec{r}') = \sum_{nm} \frac{G_{nm}^\sigma(z, z')}{2\pi \|\cdot\|_{nm}} \phi_{nm}^{j\sigma}(r) \phi_{nm}^{j'\sigma*}(r') e^{in(\theta-\theta')} \quad (5)$$

with the norm

$$\|\cdot\|_{nm} = \int_0^{R_0} \phi_{nm}^{j\sigma}(r) \phi_{nm}^{j'\sigma*}(r) r dr, \quad (6)$$

and $G_{nm}^\sigma(z, z')$ is the solution of the equation

$$\left[- \left(\frac{\nu_{nm}^{j\sigma}}{R_0} \right)^2 + \frac{2M}{\hbar^2} E + \frac{\partial^2}{\partial z^2} \right] G_{nm}^\sigma(z, z') = \frac{2Ma_0}{\hbar^2} \delta(z-z'). \quad (7)$$

The complex numbers $\nu_{nm}^{j\sigma}$ are specified by the condition of the jump of the first derivative of the Green function at $r=r_0$. For the case of weak surface scattering we get

$$\nu_{nm}^{j\sigma} = \nu_{nm}^{(0)} + \kappa_{nm}^{j\sigma}, \quad (8)$$

where $\nu_{nm}^{(0)}$ is the m th root of the Bessel function $J_n(r)$ and

$$\kappa_{nm}^{j\sigma} \approx \frac{2MV^{j\sigma}a_0}{\hbar^2} \frac{a_0}{R_0} \nu_{nm}^{(0)} \left(1 + \frac{2MV^{j\sigma}a_0}{\hbar^2} \right). \quad (9)$$

The eigenfunctions $\phi_{nm}^{j\sigma}(r)$ and $\phi_{n,m'}^{j'\sigma*}(r)$ form the biorthogonal system only for $j=j'$. Therefore, in the general case one obtains a more complicated structure of the Green function if compared with the case of an ideal surface.²¹

III. CONDUCTIVITY AND GMR

The expression for the current of electrons with spin projection σ along the wire axis takes the following form in the framework of the Kubo formalism:

$$j_z^\sigma(r, \theta, z) = \frac{4}{\pi} \frac{e^2}{\hbar} \left(\frac{\hbar^2}{2m} \right)^2 \int [G^\sigma(\vec{r}, \vec{r}') - (G^\sigma)^*(\vec{r}, \vec{r}')] \times \vec{\nabla}_z \vec{\nabla}_{z'} [G^\sigma(\vec{r}', \vec{r}) - (G^\sigma)^*(\vec{r}', \vec{r})] \times \varepsilon(r', \theta', z') r' dr' d\theta' dz', \quad (10)$$

where $\vec{\nabla}_z = \frac{1}{2}(\vec{\nabla}_z - \vec{\nabla}_{z'})$. We need to add the so-called vertex corrections when calculating the conductivity. It was shown, however,²² that this correction is equivalent to the introduction of an effective internal coordinate-dependent electrical field ε in such a way as to provide the nondivergence condition for the current, averaged over the wire cross section,

$$J^\sigma(z) = \int j_z^\sigma(r, \theta, z) r dr d\theta. \quad (11)$$

Whereas for a laterally infinite multilayer¹⁸ as well as for a segmented nanowire with ideal surface in which the effective fields can be chosen constant in each layer (respectively,

segment), the complexity of an exact Green function for a nanowire with rough surface would drastically hamper the construction of the corresponding effective fields. Fortunately, however, it can be shown numerically that a constant effective field in each segment still provides a rather good approximation. Assuming thus constant fields $\varepsilon^{j\sigma}$ in each segment j we obtain the following expression for the current:

$$\begin{aligned}
 J^{1\sigma}(z) &= \sum_{nm} \left\{ \frac{\varepsilon^{1\sigma}}{d_{nm}^{1\sigma}} + e^{2d_{nm}^{1\sigma}z} \left[-\frac{\varepsilon^{1\sigma}}{d_{nm}^{1\sigma}} + \frac{\varepsilon^{3\sigma}}{d_{nm}^{3\sigma}} \right] \right\}, \\
 J^{2\sigma}(z) &= \sum_{nm} \left\{ \frac{\varepsilon^{2\sigma}}{d_{nm}^{2\sigma}} + e^{2d_{nm}^{2\sigma}z} \left[\frac{\varepsilon^{3\sigma}}{d_{nm}^{3\sigma}} - \frac{\varepsilon^{2\sigma}}{d_{nm}^{2\sigma}} \right] \right. \\
 &\quad \left. + e^{-2d_{nm}^{2\sigma}z} \left[\frac{\varepsilon^{1\sigma}}{d_{nm}^{1\sigma}} - \frac{\varepsilon^{2\sigma}}{d_{nm}^{2\sigma}} \right] \right\}, \\
 J^{3\sigma}(z) &= \sum_{nm} \left\{ \frac{\varepsilon^{3\sigma}}{d_{nm}^{3\sigma}} + e^{-2d_{nm}^{3\sigma}z} \left[\frac{\varepsilon^{1\sigma}}{d_{nm}^{1\sigma}} - \frac{\varepsilon^{3\sigma}}{d_{nm}^{3\sigma}} \right] \right\}.
 \end{aligned} \tag{12}$$

If one chooses the effective fields as

$$\varepsilon^{j\sigma} = \varepsilon^{\sigma(0)} \left(\sum_{nm} \frac{1}{d_{nm}^{j\sigma}} \right)^{-1}, \tag{13}$$

numerical calculations show that the deviation of the current $J(z)$ from a constant is less than 1.5%. The quantity $\varepsilon^{\sigma(0)}$ is given by the total voltage across the nanowire. It is constant for all three segments but it depends on electron spin. Once the fields $\varepsilon^{j\sigma}$ are defined and the total voltage is fixed, the currents and resistivities can be calculated

$$R(\sigma_1, \sigma_2) = \frac{U^\uparrow U^\downarrow}{U^\uparrow + U^\downarrow}, \tag{14}$$

where we put the current of spin-up electrons $J^\uparrow = 1$ and

$$U^\sigma = \sum_{j=1,2,3} \varepsilon^{j\sigma}.$$

Next, the GMR can be calculated from the resistivities for parallel [$R(\uparrow\uparrow)$] and antiparallel [$R(\uparrow\downarrow)$] magnetizations of the ferromagnetic segments

$$\frac{\Delta R}{R} = \frac{R(\uparrow\downarrow) - R(\uparrow\uparrow)}{\min\{R(\uparrow\uparrow), R(\uparrow\downarrow)\}}. \tag{15}$$

In the case of weak scattering the difference to the case of an ideal lateral interface ($V^{j\sigma} \equiv 0$) is given by the z component of the electron momentum that equals

$$Q_{nm}^{j\sigma} = \sqrt{(k_F^{j\sigma})^2 - \left(\frac{\nu_{nm}^{(0)} + \kappa_{nm}^{j\sigma}}{R_0} \right)^2} + \frac{2ik_F^{j\sigma}}{l^{j\sigma}}. \tag{16}$$

Therefore the imaginary part of the momentum has the form

$$\begin{aligned}
 d_{nm}^{j\sigma} &= \text{Im} Q_{nm}^{j\sigma} \approx \frac{k_F^{j\sigma}}{l^{j\sigma}} + \frac{(\text{Im} \kappa_{nm}^{j\sigma}) \nu_{nm}^{(0)}}{R_0^2} \\
 &\quad \sqrt{(k_F^{j\sigma})^2 - \left(\frac{\nu_{nm}^{(0)}}{R_0} \right)^2} \\
 &\approx \frac{k_F^{j\sigma}}{l^{j\sigma}} + \frac{2M \text{Im}[V^{j\sigma}] a_0^2 (\nu_{nm}^{(0)})^2}{\hbar^2 R_0^3} \\
 &\quad \sqrt{(k_F^{j\sigma})^2 - \left(\frac{\nu_{nm}^{(0)}}{R_0} \right)^2}; \tag{17}
 \end{aligned}$$

evidently, for a given surface roughness its influence decreases for increasing wire radius R_0 .

We can get the classical size effect for a nonsegmented paramagnetic wire using Eq. (17). It is seen from the expression for the current (12) that the conductivity is proportional to the sum

$$\sum_{nm} \frac{1}{d_{nm}^{j\sigma}}.$$

For a large nanowire radius R_0 we can replace the sum by the integral

$$\begin{aligned}
 &\int_{x^2+y^2 < (k_F^{j\sigma})^2} \gamma(x,y) \sqrt{(k_F^{j\sigma})^2 - (x^2+y^2)} \Big/ \\
 &\quad \times \left(\frac{k_F}{l} + \frac{2M \text{Im}[V^{j\sigma}] a_0^2}{\hbar^2 R_0} (x^2+y^2) \right) dx dy, \tag{18}
 \end{aligned}$$

where the function $\gamma(x,y)$ is the density of the Bessel functions zeros $\nu_{nm}^{(0)}$. For small values of the surface potential the surface contribution to the resistivity decreases as $1/R_0$ in accordance with the quasiclassical treatment of the surface-roughness problem.⁹

There is another source of the dependence of conductivity and GMR on the cross section, namely the necessary renormalization of the Fermi momenta.²³ We equate the total (s and d) electron concentration $n = 2n_s + n_d^\uparrow + n_d^\downarrow$ in an infinite volume to the concentration of electrons in a finite-size sample. Here n_s is the one-half concentration of s electrons and n_d^σ is the concentration of d electrons with spin σ . The electron concentrations are given by

$$n_{s,d}^\sigma = -\text{Im} \frac{1}{\pi} \frac{1}{abc} \int \int G^\sigma(\vec{r}, \vec{r}, E) d^3 r dE. \tag{19}$$

The resulting $k_F^{j\sigma}$ values are then used to calculate the mean free path of the s electrons

$$\frac{l^\sigma(R_0)}{l^\sigma(R_0 \rightarrow \infty)} = \frac{\rho_d^\sigma(R_0 \rightarrow \infty)}{\rho_d^\sigma(R_0)}.$$

Note that both the density of states ρ_d^σ and the mean free paths of s electrons oscillate with different periods as a function of nanowire cross section due to the different Fermi momenta of d electrons with opposite spins.

Turning back to Eq. (17) we note that the interplay between bulk and surface scattering is explicitly seen in this formula. There are two limiting cases for which the effective fields can be estimated; in the case of specular surface reflection $V^{j\sigma} \equiv 0$, we see that

$$\varepsilon^{j\sigma} \sim 1/l^{j\sigma}, \quad (20)$$

while for the case of infinitely long mean free paths,

$$\varepsilon^{j\sigma} \sim \text{Im } V^{j\sigma}; \quad (21)$$

summarizing over indices n, m such that

$$[\nu_{nm}^{(0)}/R_0]^2 < (k_F^{j\sigma})^2,$$

we see from Eq. (17) that the surface contribution to the resistivity decreases as R_0^{-1} .

IV. RESULTS AND DISCUSSION

We constructed the exact one-electron Green function for the segmented nanowire based on Eq. (1), but for the sake of simplicity the numerical calculations were performed for the case of weak surface scattering,

$$\frac{2M \text{Im } V^{j\sigma} a_0}{\hbar^2} \ll 1.$$

At sufficiently low temperatures we may neglect electron-phonon and electron-magnon scattering. The GMR is then solely determined by the spin-dependent electron scattering in the bulk and on the interfaces. In the present consideration we focus on the spin-dependent lateral (outer) surface scattering and neglect the electron scattering on the (inner) interfaces between the segments of the wire. Figure 1 shows the GMR as a function of the segmented nanowire radius R_0 for mean free paths l^\uparrow and l^\downarrow obtained for Co and Py layered wires⁸ and an ideal lateral surface. For small and decreasing nanowire cross section the GMR displays large and increasing oscillations. This can be easily explained if we take into account that the GMR is controlled by the spin polarization of the current, which (for a negligibly small thickness of the paramagnetic spacer) is proportional to the ratio $(l^\uparrow - l^\downarrow)^2 / (l^\uparrow l^\downarrow)$. The mean free paths of the s electrons are defined by the DOS of d electrons via s - d scattering. Since l^\uparrow and l^\downarrow oscillate with different periods this ratio oscillates as well and thus can produce high values, while for $k_F^\uparrow \approx k_F^\downarrow$ (for d electrons) the GMR would be almost constant. These dependencies have thus to be considered as a complicated superposition of oscillating spin-up and spin-down d -electrons' densities of states. As expected, the GMR oscillation becomes more pronounced for decreasing nanowire dimensions. The interplay between *bulk* mean free paths l^\uparrow and l^\downarrow defines the amplitude of the oscillations and the limiting value of the GMR as the nanowire radius increases.

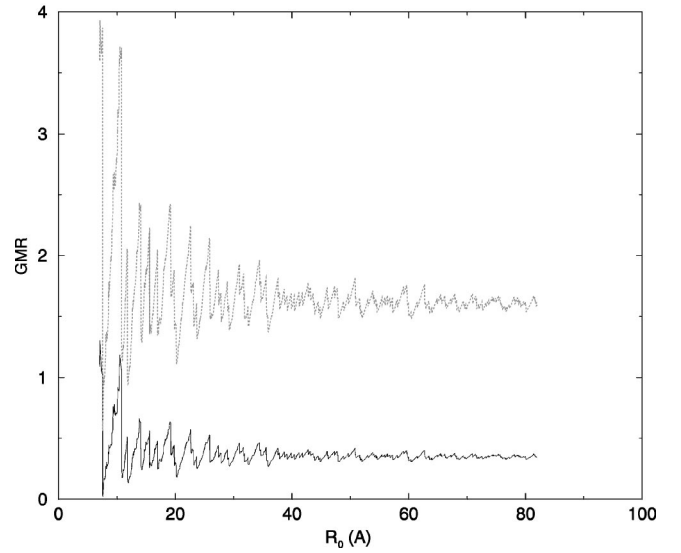


FIG. 1. GMR in a segmented cylindrical nanowire with ideal lateral surface as a function of the nanowire radius. Segment length $c_1 = c_3 = 300.0$, $c_2 = 7.0$ Å; $k_F^\uparrow = 1.40$, $k_F^\downarrow = 0.40$, $k_F^s = 1.20$ Å⁻¹; $l^\uparrow = 40.0$, $l^\downarrow = 120.0$ Å (solid line), and $l^\uparrow = 13.0$, $l^\downarrow = 120.0$ Å (dotted line). The values for the curves refer to Co and Py segmented wires, respectively. For the notations compare Ref. 23.

Before further considering the interplay between the influence of bulk and surface scattering on the GMR, we present the calculations of the resistivity of a single paramagnetic nanowire. The size effect for the resistivity of the paramagnetic wire is demonstrated in Fig. 2. Qualitatively it is similar to the size effect found in Ref. 10, although the

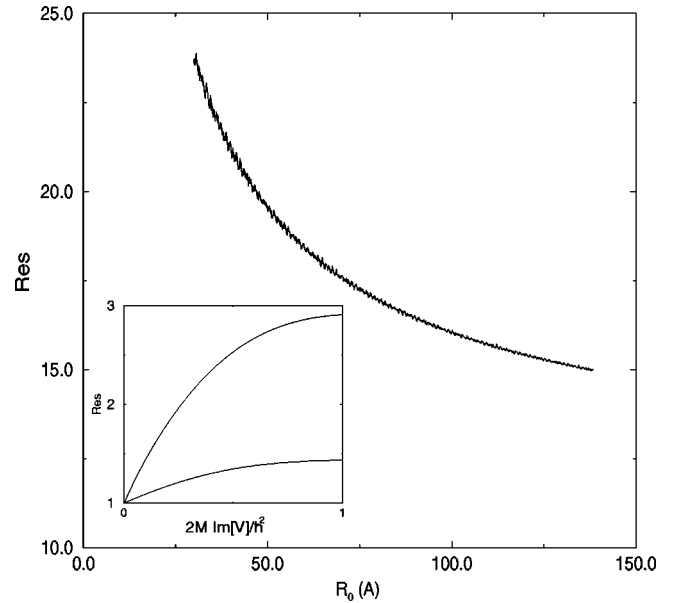


FIG. 2. Resistivity (arbitrary units) of a single paramagnetic wire as a function of the nanowire radius, $l^\uparrow = l^\downarrow = 600.0$ Å, $k_F^s = 1.20$, $2M \text{Im}[V]/\hbar^2 = 0.5$ Å⁻¹. In the panel the normalized resistivity of a single paramagnetic wire as a function of surface potential is represented as $l^\uparrow = l^\downarrow = 120.0$ Å, $k_F^s = 1.20$ Å⁻¹ for $R_0 = 20$ Å (upper curve), and $R_0 = 100$ Å (lower curve).

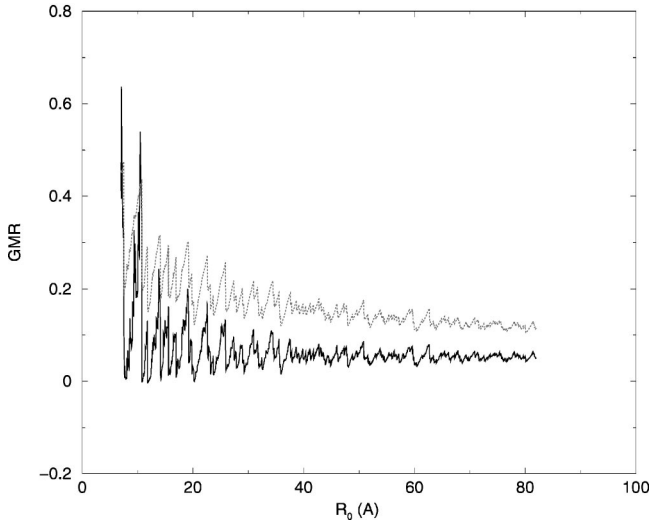


FIG. 3. Increase of the GMR in a segmented cylindrical nanowire due to spin dependent surface scattering of the electrons. $c_1 = c_3 = 300.0$, $c_2 = 5.0 \text{ \AA}$; $l^\uparrow = 160$, $l^\downarrow = 240.0 \text{ \AA}$; $k_F^\uparrow = 1.40$, $k_F^\downarrow = 0.40$, $k_F^s = 1.20 \text{ \AA}^{-1}$; $2M \text{Im}[V_1]/\hbar^2 = 2M \text{Im}[V_2]/\hbar^2 = 2M \text{Im}[V_3]/\hbar^2 = 0$ (solid line); $2M \text{Im}[V_1]/\hbar^2 = 0.6$, $2M \text{Im}[V_2]/\hbar^2 = 1.2$, $2M \text{Im}[V_3]/\hbar^2 = 0.12 \text{ \AA}^{-1}$ (dotted line).

k_F^- and ρ^- renormalization taken into account in our consideration results in a weakly oscillating R dependence. On the panel the dependencies of the resistivity of a nonsegmented paramagnetic nanowire on the strength of the surface scattering are shown. Not unexpectedly the resistivity increases as the surface scattering grows and the increase is stronger for a smaller radius of the nanowire.

The GMR in a segmented nanowire with spin-dependent diffusive electron scattering on the surface displays a great diversity in its behavior. The surface contribution to the spin-dependent scattering can either magnify the difference between the effective scattering rates of electrons with different spins $d_{nm}^{j\uparrow}$ and $d_{nm}^{j\downarrow}$ or decrease it. Depending on the strength of the surface scattering it can lead to both an increase or decrease of the GMR. Comparing the curves in Fig. 3 one can see that if the spin asymmetry $(l^\downarrow/l^\uparrow - 1)$ of the bulk scattering is much smaller than the asymmetry $(\text{Im} V_1/\text{Im} V_3 - 1)$ of the surface scattering, the GMR in the sample with surface scattering is much higher ($\sim 2-3$ times) than in the sample with ideal lateral surface even for wire diameters comparable to the mean free path.

If the spin asymmetry is smaller for surface scattering and the amplitude of the surface scattering rate is high enough the average value of the GMR decreases (Fig. 4). From this figure we notice that the surface scattering can also significantly decrease the amplitude of the oscillations of the GMR.

Finally, if the spin asymmetries of the surface and bulk scattering have different signs, the contribution of surface scattering tends to equalize the effective scattering rates d^\uparrow and d^\downarrow , and the GMR shows a pronounced drop in the region of small radii, where the surface influence is particularly strong (Fig. 5).

Based on these results we conclude that surface scattering provides an important contribution to the experimentally ob-

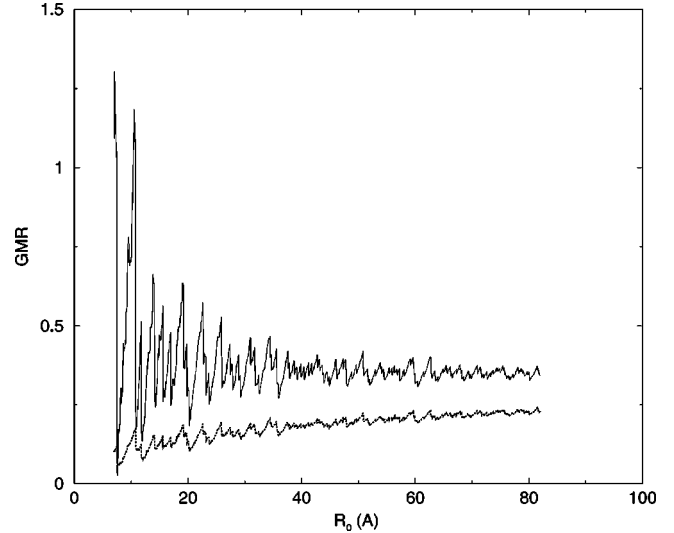


FIG. 4. Decrease of the GMR due to spin dependent surface scattering of the electrons. $c_1 = c_3 = 300.0$, $c_2 = 5.0 \text{ \AA}$; $l^\uparrow = 40$, $l^\downarrow = 120.0 \text{ \AA}$; $k_F^\uparrow = 1.40$, $k_F^\downarrow = 0.40$, $k_F^s = 1.20 \text{ \AA}^{-1}$; $2M \text{Im}[V_1]/\hbar^2 = 2M \text{Im}[V_2]/\hbar^2 = 2M \text{Im}[V_3]/\hbar^2 = 0$ (solid line); $2M \text{Im}[V_1]/\hbar^2 = 0.9$, $2M \text{Im}[V_2]/\hbar^2 = 0.7$, $2M \text{Im}[V_3]/\hbar^2 = 0.5 \text{ \AA}^{-1}$ (dotted line).

served difference of the GMR in multilayers and segmented nanowires.⁸ We may note that in a segmented nanowire consisting of homogeneous material with a low concentration of impurities (like, e.g., Co) the spin asymmetry of the surface scattering may not differ too much from its value for bulk scattering, whereas in the case of the alloy Py a redistribution of the atoms (constituents of the alloy) near the surface can magnify the asymmetry. Correspondingly the GMR will decrease in the first case and increases in the second case.

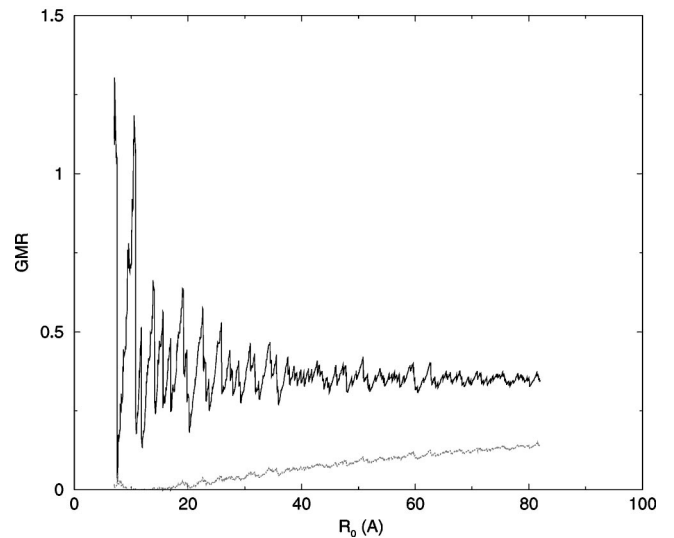


FIG. 5. The suppression of the GMR in the case when the surface scattering tends to equalize the mean free paths for spin-up and spin-down electrons. $c_1 = c_3 = 300.0$, $c_2 = 5.0 \text{ \AA}$; $l^\uparrow = 40$, $l^\downarrow = 120.0 \text{ \AA}$; $k_F^\uparrow = 1.40$, $k_F^\downarrow = 0.40$, $k_F^s = 1.20 \text{ \AA}^{-1}$; $2M \text{Im}[V_1]/\hbar^2 = 2M \text{Im}[V_2]/\hbar^2 = 2M \text{Im}[V_3]/\hbar^2 = 0$ (solid line); $2M \text{Im}[V_1]/\hbar^2 = 0.15$, $2M \text{Im}[V_2]/\hbar^2 = 0.4$, $2M \text{Im}[V_3]/\hbar^2 = 0.5 \text{ \AA}^{-1}$ (dotted line).

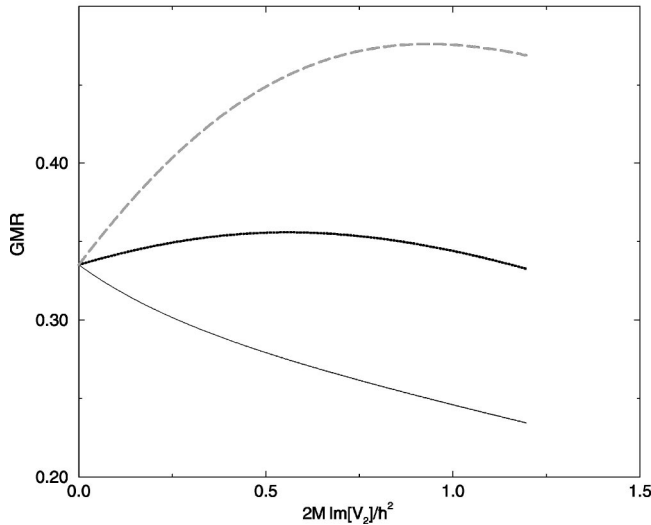


FIG. 6. GMR as a function of the surface potential. $c_1=c_3=700.0$, $c_2=7.0$ Å; $k_F^{\uparrow}=1.40$, $k_F^{\downarrow}=0.40$, $k_F^s=1.20$ Å $^{-1}$; $l^{\uparrow}=40.0$, $l^{\downarrow}=120.0$ Å; $R_0=30$ Å; $\text{Im}[V_1]:\text{Im}[V_2]:\text{Im}[V_3]=3:4:1.5$ (solid line), $\text{Im}[V_1]:\text{Im}[V_2]:\text{Im}[V_3]=4:4:1.0$ (heavy dotted line), $\text{Im}[V_1]:\text{Im}[V_2]:\text{Im}[V_3]=5:4:0.5$ (heavy broken line).

Finally, we present in Fig. 6 the dependence of the GMR on $V^{j\sigma}$ for a fixed radius (30 Å). For each curve the ratio between the spin components of the surface potential is fixed. It can be seen from this figure that the GMR for the fixed radius can increase as well as decrease or may be a nonmonotonic function of the surface-potential strength. The behavior of the curves is determined mainly by the difference in the spin-up and spin-down surface potential.

V. CONCLUSION

We have developed a Green-function-based quantum statistical approach to the GMR in segmented nanowires,

thereby including spin-dependent diffusive surface scattering. We have constructed the Green function and calculated the resistivity and the GMR of the nanowire. The interplay between the spin-dependent electron scattering in the bulk and in the surface leads to a complex behavior of the GMR as a function of nanowire radius and surface potential strength. Our approach reproduces the size effect obtained in quasiclassical theories. The GMR has been found to oscillate due to the quantization of the electron motion in the direction perpendicular to the wire axis. The theory of the GMR developed here suggests that the spin-dependent surface electron scattering significantly changes the value of the GMR in segmented nanowires if compared with infinite multilayers. This change is caused by the interplay between the bulk and the surface spin-dependent electron scattering. In particular, the surface scattering reduces the amplitude of the GMR oscillations with the nanowire radius. Our analysis suggests that a high GMR may be obtained by using a thin segmented nanowire of a ferromagnetic metal with high conductivity (for example, iron), coated by a thin layer of a nonmagnetic metal (for example, Cr), which produces a lateral interface with large spin asymmetry of the interfacial scattering. Such a structure may be considered as a combination of structures with current in plane and current perpendicular to the plane geometries. We restricted our consideration to the case of weak surface scattering, but qualitatively our analysis is also correct for a wider range of surface potential.

ACKNOWLEDGMENTS

A. V. Vedyayev acknowledges the CENG DRMC SP2M for hospitality and the Russian Foundation of Fundamental Research for financial support. M. Ye. Zhuravlev is grateful to Bielefeld University for hospitality. This work has been supported by the Deutsche Forschungsgemeinschaft in the ‘‘Forschergruppe Nanometer-Schichtsysteme.’’

*On leave from the Institute of General and Inorganic Chemistry, RAS, Leninskii prosp., 31, Moscow 117907, Russian Federation.

[†]On leave from Physical Department of Moscow State University, Moscow 119899, Russian Federation.

¹M. N. Baibich, J. M. Broto, A. Fert, F. Nguyen Van Dau, F. Petroff, P. Etienne, G. Creuzet, A. Friederich, and J. Chazelas, *Phys. Rev. Lett.* **61**, 2472 (1988); G. Binasch, P. Grunberg, F. Saurenbach, and W. Zinn, *Phys. Rev. B* **39**, 4828 (1989).

²J. Magn. Magn. Mater. **198-199** (1999); **200** (1999).

³T. Valet and A. Fert, *Phys. Rev. B* **48**, 7099 (1993).

⁴P. M. Levy, S. Zhang, and A. Fert, *Phys. Rev. Lett.* **65**, 1643 (1990); H. E. Camblong, P. M. Levy, and S. Zhang, *Phys. Rev. B* **51**, 16 052 (1995).

⁵H. E. Camblong, S. Zhang, and P. M. Levy, *Phys. Rev. B* **47**, 4735 (1993).

⁶A. Vedyayev, C. Cowache, N. Ryzhanova, and B. Dieny, *J. Phys.: Condens. Matter* **5**, 8289 (1993).

⁷A. Vedyayev, N. Ryzhanova, B. Dieny, P. Dauguet, P. Gandit, and J. Chaussy, *Phys. Rev. B* **55**, 3728 (1997).

⁸A. Fert and L. Piraux, *J. Magn. Magn. Mater.* **200**, 338 (1999).

⁹L. A. Falkovsky, *Adv. Phys.* **32**, 753 (1983).

¹⁰Z. Tešanović, M. Jarić, and S. Maekawa, *Phys. Rev. Lett.* **57**, 2760 (1986); L. Sheng, D. Y. Xing, and Z. D. Wang, *Phys. Rev. B* **51**, 7325 (1995); G. Palasantzas and J. Barnas, *ibid.* **56**, 7726 (1997).

¹¹K. M. Schep, P. J. Kelly, and G. E. W. Bauer, *Phys. Rev. B* **57**, 8907 (1998).

¹²W. H. Butler, X. G. Zhang, D. M. C. Nicholson, and J. M. Macclaren, *Phys. Rev. B* **52**, 13 399 (1995).

¹³E. Yu. Tsymlal and D. G. Pettifor, *Phys. Rev. B* **54**, 15 314 (1996).

¹⁴M. D. Stiles, *J. Appl. Phys.* **79**, 5805 (1996).

¹⁵J. Mathon, *Phys. Rev. B* **55**, 960 (1997).

¹⁶A. Fert and I. A. Campbell, *J. Phys. F: Met. Phys.* **6**, 849 (1976).

¹⁷F. Brouers, A. Vedyayev, and M. Giorgino, *Phys. Rev. B* **7**, 380 (1973).

¹⁸A. Vedyayev, M. Chshiev, N. Ryzhanova, B. Dieny, C. Cowache, and F. Brouers, *J. Magn. Magn. Mater.* **172**, 53 (1997).

¹⁹S. Zhang and P. Levy, *Phys. Rev. Lett.* **77**, 916 (1996).

²⁰E. A. Coddington and N. Levinson, *Theory of Ordinary Differen-*

tial Equations (McGraw-Hill, New York, 1955).

²¹The details of our calculation of the exact Green function can be found in <http://www.Physik.Uni-Bielefeld.DE/experi/d0/lutz.htm> or are available on request.

²²P. M. Levy, H. E. Camblong, and S. Zhang, *J. Appl. Phys.* **75**, 7076 (1994).

²³In the calculations we supposed that the Fermi momenta in both ferromagnetics depend only on the spin projection of the electron relative to the magnetization. Therefore, we use two parameters $k_F^{\uparrow,\downarrow}$ for the Fermi momenta of d electrons with spin direction parallel (spin-up) and antiparallel (spin-down) to the

magnetization, respectively, and k_F^s for the Fermi momenta of s electrons in all three segments. For simplicity we suppose that the Fermi momentum of s electrons in the paramagnetic segment is equal to k_F^s as well. The same notations are held for the mean free paths of s electrons. The bulk values of the corresponding Fermi momenta and the mean free paths are given in the figure captions. The components of the surface potential for spin-up and spin-down s electrons are denoted by V_1 and V_3 , respectively. The value of the surface potential for s electrons in the paramagnetic spacer is designated by V_2 .